

PAPER • OPEN ACCESS

Examining the Spatial Frequency Components of a Digital Dental Detector

To cite this article: A. Anastasiou *et al* 2017 *J. Phys.: Conf. Ser.* **931** 012005

View the [article online](#) for updates and enhancements.

Examining the Spatial Frequency Components of a Digital Dental Detector

A. Anastasiou¹, C. Michail^{1,2}, V. Koukou², N. Martini², A. Bakas^{2,3}, F. Papastamati¹, P. Maragkaki¹, L. Lavdas^{2,3}, G. Fountos^{1,2}, I. Valais^{1,2}, N. Kalyvas^{1,2*}

¹Department of Biomedical Engineering, Technological Educational Institute of Athens GREECE

²Laboratory of Radiation Physics, Materials Technology and Biomedical Imaging, Faculty of Technological Applications, Technological Educational Institute of Athens, GREECE.

³Department of Radiology and Radiation Therapy, Technological Educational Institute of Athens, GREECE

*email: nkalyvas@teiath.gr

Abstract. Digital X-ray detectors are widely used in dental radiography. The scope of this work is the examination of the spatial frequency component of a dedicated dental CMOS detector. A commercially available SCHICK CDR CMOS detector was irradiated at a Del Medical Eureka X-ray system at 60kVp and 70kVp. The irradiation setup included images of an edge, for Modulation Transfer Function (MTF) calculation. The air-KERMA was measured with an RTI PIRANHA X-ray multimeter. The images were evaluated in 'for presentation' format with the use of ImageJ software. The linear range of the detector was found in the range 13 μ Gy-183 μ Gy at 60 kVp and 18 μ Gy-180 μ Gy at 70 kVp. By inspecting the MTF curves it was found that MTF(6lp/mm)60kVp=0.29 and MTF(6lp/mm)70kVp=0.25. The inspection of the Normalized Noise Power Spectrum (NNPS) showed similar low noise components. Our results indicate that this detector presents comparable performance at both kVp, although its X-ray response (pixel value vs air KERMA) was not equal to previously published results, for the same detector type.

Keywords: dental detector; image quality; CMOS; MTF; NNPS

1. Introduction

Dental X-ray imaging, is a valuable tool for assessing teeth condition and evaluate treatment plans. In recent years digital detectors are used to acquire dental radiographs [1]. These are usually indirect detectors, that is a scintillator coupled to a photosensitive receptors absorbs the X-ray energy, converts it to optical photon energy of a wavelength within the photoreceptor sensitivity spectrum [2]. The performance of these digital detectors can be evaluated by simple metrics such as Pixel Value to Entrance Surface Air Kerma (ESAK) Response curve (PVR). PVR characterizes the linearity of the detector response with respect to X-ray exposure. In addition spatial frequency image quality metrics are available like MTF, demonstrating the ability of the detector to resolve objects of different dimensions, as well as, NNPS which demonstrates the relative noise components in spatial frequency domain [3,4]. In current work a digital detector SCHICK CDR CMOS was examined. In a previous work this detector type but with a different serial number was examined in terms of PVR and noise [5]. In this work we extend our research by including a more thorough investigation of the spatial frequency components like MTF and NNPS at a detector of the same type but with a different serial number. The results showed that this detector demonstrated similar performance at 60 kVp and 70 kVp.

2. Materials and Methods

2.1. Detector type



Content from this work may be used under the terms of the [Creative Commons Attribution 3.0 licence](https://creativecommons.org/licenses/by/3.0/). Any further distribution of this work must maintain attribution to the author(s) and the title of the work, journal citation and DOI.

A SHICK CDR CMOS indirect detector with serial number 540957 was examined. The detector utilizes an active pixel sensor (APS) and a pixel size of $40\ \mu\text{m}$. The images were collected automatically created in the accompanied software in 8 bit depth ‘for presentation’ mode, directly available for observation, incorporating all possible image processing algorithms suggested by the vendor. The raw image data were available.

2.2. Irradiation conditions

The detector was irradiated with 60 kVp and 70 kVp X-ray spectra by using a del Medical Eureka X-ray system. The ESAK was measured with an RTI PIRANHA X-ray multimeter. For the calculation of PVR and NNPS uniformly exposed images were obtained. For the MTF calculation, images of an irradiated tungsten slanted edge test device, supplied by the PTW Freiburg Company, were obtained [3,4].

2.3. Evaluation method

PVR for both kVp settings was evaluated by calculating the mean pixel value, measured by ImageJ software, against the measured ESAK, which was found ranging between $13\ \mu\text{Gy}$ to $183\ \mu\text{Gy}$. For MTF calculation an Edge Spread Function (ESF) was obtained by the slanted edge image. ESF was then differentiated to obtain the Line Spread Function (LSF). Finally the Fast Fourier Transform (FFT) of LSF, normalized to zero spatial frequency provided MTF. NNPS was calculated by selecting a uniform image at an X-ray exposure corresponding to the linear range of the detector. Region of Interests (ROIs) were then taken and from each ROI a matrix of signal variations was acquired. A 2D-FFT of each ROI was calculated and added to the NPS ensemble. NNPS was obtained by dividing NPS by the square of the corresponding mean signal value. Afterwards the ensemble average was calculated. A more detailed account for NNPS and MTF calculation can be obtained in literature [3,4]. For calculation purposes the ImageJ plug-in COQ was utilized [6,7].

3. Results and Discussion

In figure 1 the calculated PVR of the detector studied is demonstrated. It can be observed that the response of the detector ‘for presentation’ operation mode is similar for both kVp. In addition a linear range can be distinguished between $18\ \mu\text{Gy}$ to $144\ \mu\text{Gy}$. By comparing these PVR with a previous work, for another SCHICK CMOS detector [5] we found that at 60 kVp the gradient of the curve was similar, but with different zero exposure offset values and at 70 kVp the PVR presented in this work demonstrate a slightly higher gradient. The differences between this work and that of reference 5, may be attributed to the different exposure conditions setup [5], which did not allow very low dose evaluation.

In figure 2 the calculated MTF curves for 60 kVp and 70 kVp, for spatial frequencies up to 120 cycles/cm (1 cycle/cm = 10 cycles/mm) are demonstrated. It can be observed that the calculated curves are very similar implying that the higher energies of the 70 kV spectrum do not produce enough absorption effects near the phosphor exit so as to enhance the MTF curve. On the contrary, by calculating the area over the MTF curve $S = \sum_f MTF(f)$ it can be found that $S_{60\text{ kV}} = 37.59$ cycles/mm

and $S_{70\text{ kV}} = 36.09$ cycles/mm, meaning that the signal transfer capability of the detector studied at 60 kVp is slightly better. In addition the 10% MTF is approximately at 10 cycles/mm for 70 kVp. This value is higher than what has been reported in literature that is 10% MTF at 6 cycles/mm for a CMOS/Gd₂O₂S:Eu (65.1 mg/cm²) combination [3]. However other CMOS/scintillator combinations such as CMOS/Gd₂O₂S:Eu (33.3 mg/cm²) and CMOS/Lu₂O₃:Eu (65.1 mg/cm²) demonstrates 10% MTF above 11 cycles/mm [4]. The exposure conditions in these cases were not exactly the same since the 70kVp X-ray spectrum was hardened by the addition of 21 mm Al [3,4] Other dental detectors, by means of viewing the image of a bar pattern, have reported a resolution limit above 10 cycles/mm [8].

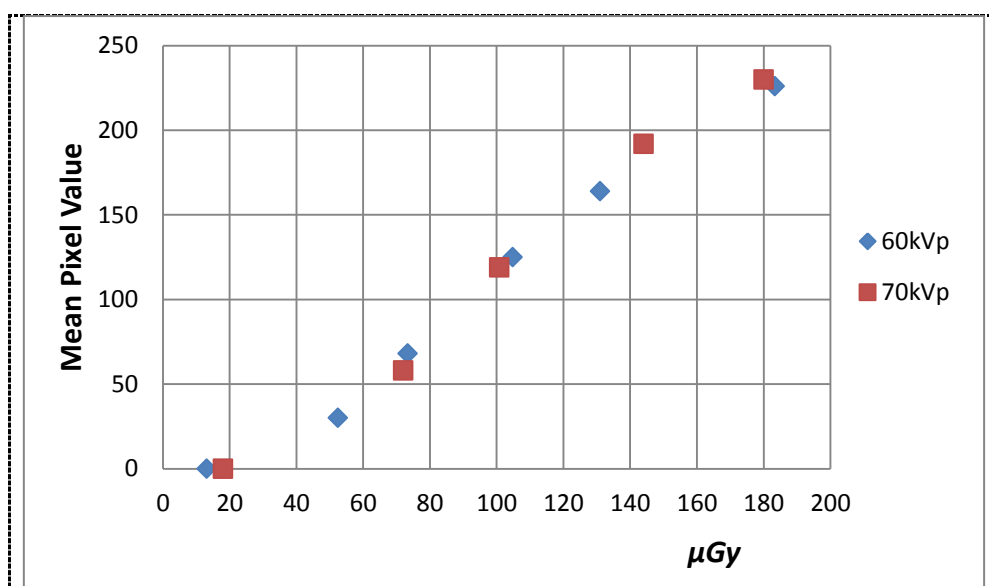


Figure 1. The PVR of the detector for 60 kVp (blue rhombus) and 70 kVp (red square).

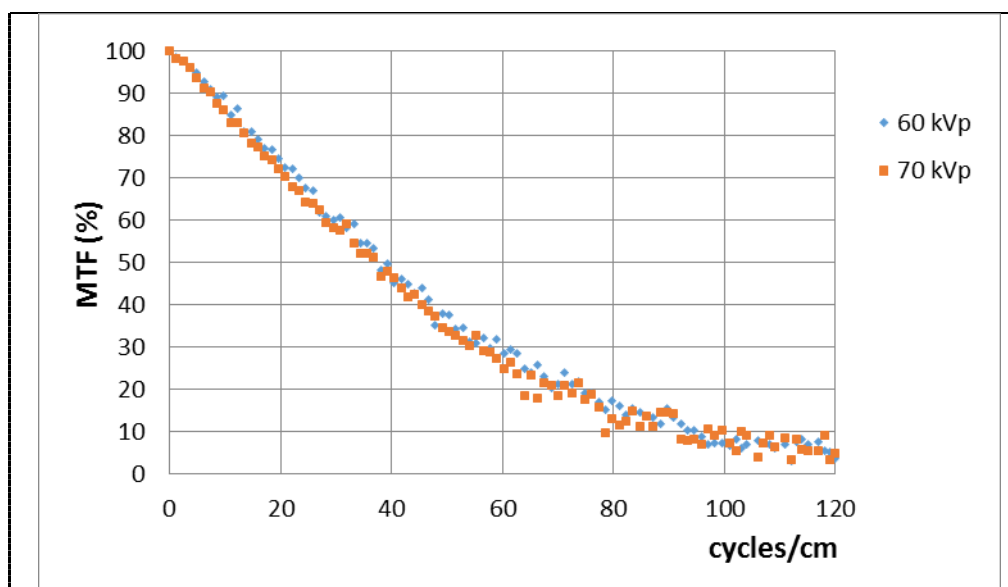


Figure 2. The MTF of the detector for 60 kVp (blue rhombus) and 70 kVp (red square).

In figure 3 the NNPS curves at 60 kVp, 104.8 μGy and 70 kVp, 100.8 μGy are demonstrated. It may be seen that the 70 kV irradiation conditions exhibit higher noise. This may be explained by taking into account that: (a) the 70 kVp X-rays demonstrate lesser probability of absorption in the scintillator material and (b) the ESAK at 70 kVp is by 4 μGy lower. Both these factors yield poorer image statistics in the 70 kVp case, thus the relative noise is expected to be higher. It is of interest to notice however that the resulted images were in ‘for presentation’ mode, which includes the effect of the software bit manipulation of the detector. Thus NNPS evaluation included the effects of signal processing algorithms [9,10].

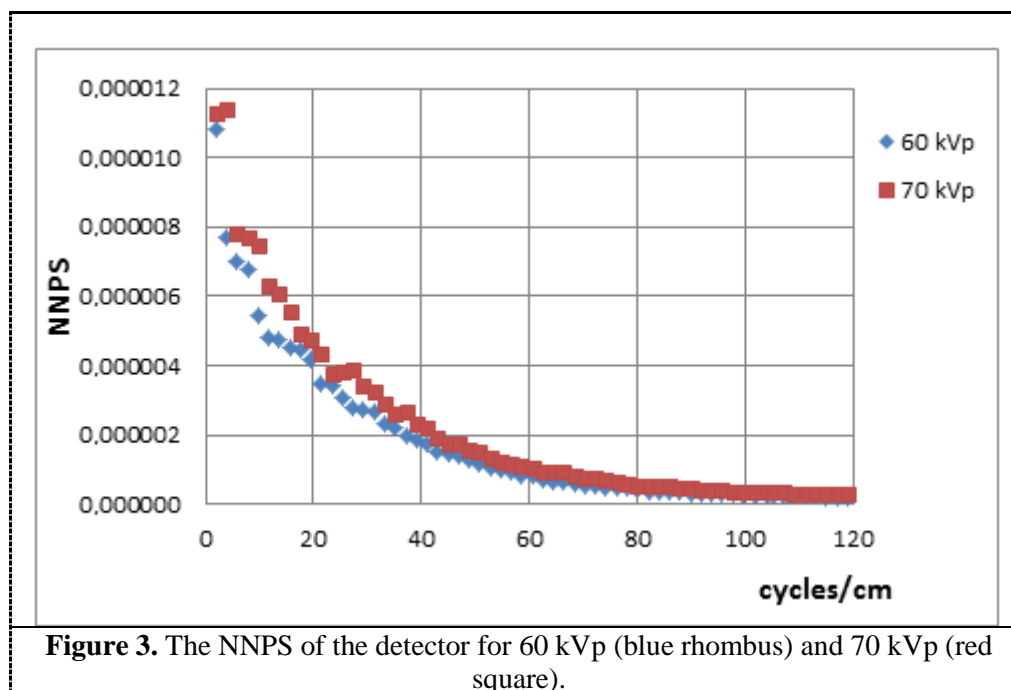


Figure 3. The NNPS of the detector for 60 kVp (blue rhombus) and 70 kVp (red square).

4. Conclusion

A digital dental detector was evaluated in terms of PVR, MTF and NNPS at 60 kVp and 70 kVp irradiation conditions. It was found that the detector presents comparable performance in both kVp settings.

5. References

- [1] Manousaridis G, Tsiklakis K, Stefanou E, Yakoumakis E, Hourdakakis C, Kamenopoulou V 2015 *Odontostomatological Progress* **69**, 212.
- [2] Kandarakis I S 2016 *J. Lumin* **169** 553.
- [3] Seferis I E, Michail CM, Valais IG, Fountos G P Kalyvas N I, Stromatia F, Oikonomou G, Kandarakis I S and Panayiotakis GS 2013 *Nucl. Instrum. Meth. Phys. Res. A* **729** 307.
- [4] Seferis I, Michail C, Valais I, Zeler J, Liaparinis P, Fountos G, Kalyvas N, David S, Stromatia F, Zych E, Kandarakis I and Panayiotakis G 2014 *J. Lumin.* **151** 229.
- [5] Kalyvas N, Maragkaki P, Bakas A, Fountos G Koukou V, Martini N, Michail C, Valais I, Kandarakis I 2016 *Physica Medica* **32** (Suppl 3), 286
- [6] <https://imagej.nih.gov/ij/> (last accessed August 2017).
- [7] Donini B, Rivetti S, Lanconelli N, Bertolini M, 2014 *Med. Phys.* **39** 051903-1
- [8] Farman A G, Farman T T, 2005 *OOOOE* **99**, 485 doi:10.1016/j.tripleo.2004.04.002
- [9] Michail C, Spyropoulou V, Kalyvas N, Valais I, Dimitropoulos N, Fountos G, Kandarakis I and Panayiotakis G 2009 *J. Instrum.* **4** P05018.
- [10] Michail C, Kalyvas N, Valais I, Fudos I, Fountos G, Dimitropoulos N, Koulouras G, Kandris D, Samarakou M and Kandarakis I 2014 *BioMed. Res. Int.* **2014** 634856.